

Spin-Seebeck effect in a strongly interacting Fermi gas

C. H. Wong, H. T. C. Stoof, and R. A. Duine

Institute for Theoretical Physics, Utrecht University, Leuvenlaan 4, 3584 CE Utrecht, The Netherlands

(Received 21 March 2012; published 15 June 2012)

We study the spin-Seebeck effect in a strongly interacting, two-component Fermi gas and propose an experiment to measure this effect by relatively displacing spin-up and spin-down atomic clouds in a trap using spin-dependent temperature gradients. We compute the spin-Seebeck coefficient and related spin-heat transport coefficients as functions of temperature and interaction strength. We find that, when the interspin scattering length becomes larger than the Fermi wavelength, the spin-Seebeck coefficient changes sign as a function of temperature, and hence so does the direction of the spin separation. We compute this zero-crossing temperature as a function of interaction strength and in particular in the unitary limit for the interspin scattering.

 DOI: [10.1103/PhysRevA.85.063613](https://doi.org/10.1103/PhysRevA.85.063613)

PACS number(s): 67.85.-d, 67.10.Fj, 67.10.Jn

I. INTRODUCTION

Spin caloritronics, the study of coupled spin and heat transport, is a rapidly developing subfield of spintronics [1]. In particular, the spin-dependent generalization of the Seebeck effect, called the spin-Seebeck effect, has been intensively studied in the solid-state environment [2]. Recently, there has been broad interest in exploring spintronic phenomena in cold atomic systems [3–5]. Spin transport in a strongly interacting, two-component Fermi gas was investigated experimentally in Ref. [6]. It is the purpose of this article to study the associated heat transport, i.e., thermo-spin effects, in a similar setting.

In the ordinary Seebeck effect in metals, an electrochemical potential gradient is generated by applying a temperature gradient. Similarly, for a gas with two spin states, the spin-Seebeck coefficient S_s determines the spin chemical potential μ_s generated by a spin temperature gradient ∇T_s through the relation $\nabla \mu_s = S_s \nabla T_s$, where $\mu_s \equiv \mu_+ - \mu_-$ and $T_s \equiv T_+ - T_-$, μ_σ and T_σ being the spin-dependent chemical potential and temperatures of the spin σ atoms, respectively, and we label spin components by + and -. To measure the spin-Seebeck coefficient, we propose relatively displacing the center of mass of spin-up and spin-down atom clouds in a harmonic trap by applying a spin-dependent temperature gradient, for example, by selectively heating one spin component with a laser, as illustrated in Fig. 1. The locations x_\pm of the center of mass of the spin-up and spin-down atoms are shifted to the minimum of $\mu_\pm + V$, where V is the trapping potential, resulting in a spin separation, $x_s = x_+ - x_- = S_s \nabla T_s / m\omega^2$, where m is the mass of the atoms and ω is the trap frequency in the direction of the temperature gradients. For an order of magnitude estimate, we take $S_s \simeq 0.01 k_B$, as verified below. For $\nabla T_s = 10^{-5}$ K/cm [7], $\omega = 2\pi \times 1.46$, we find $x_s \simeq 1$ mm, which is well within experimental resolution.

We have computed the spin-Seebeck coefficient for a two-component Fermi gas, plotted in Fig. 2, as a function of temperature and for several values of the interaction strength $k_F a$, where k_F is the Fermi wave vector and a is the interspin scattering length. As seen from the figure, for weak interactions ($k_F a < 1$), S_s is small and negative, while for strong interactions ($k_F a \geq 1$), S_s is larger and its sign changes as a function of temperature. In terms of the experiment mentioned above, this means that the spin displacement changes direction as a function of temperature, which is an interesting qualitative effect. We also plot the

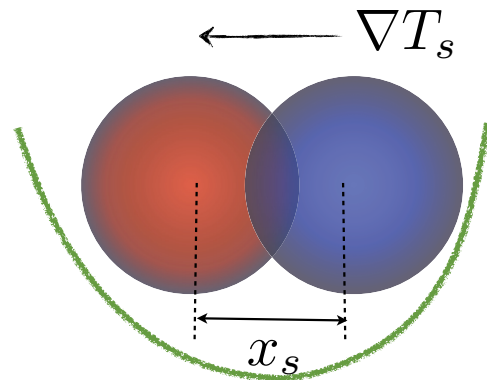


FIG. 1. (Color online) Spin-up and spin-down atomic clouds are spatially relatively displaced in the presence of a spin temperature gradient. The distance between the center of mass of the different spin components, denoted by x_s , is proportional to the spin-Seebeck coefficient.

zeros of S_s as a function of $k_F a$ in Fig. 3(d). The temperature of the zero crossing reaches a universal value, T_0 , in the unitary limit for the interspin scattering length $k_F a \rightarrow \infty$. We find $T_0 \simeq 0.378 T_F$ in our calculation, where T_F is the Fermi temperature.

The thermodynamic reciprocal of the spin-Seebeck effect is the spin-Peltier effect, in which a spin-dependent heat current proportional to the spin-Seebeck coefficient is induced by a spin current. This effect will heat up spin-up and spin-down components differently and provides another way to measure S_s . Furthermore, as discussed in Ref. [5], the spin-Seebeck effect contributes to the total dissipation so that S_s can also be measured through the heating.

We note that the spin-Seebeck coefficient was calculated for a weakly interacting Bose gas in Ref. [5], but the Bose gas is unstable toward the formation of molecules for large scattering lengths, which makes the strongly interacting regime more difficult to realize experimentally.

II. PHENOMENOLOGY

We are specifically interested in phenomena due to *spin-drag*, the transfer of momentum between different spins due to interspin scattering, which allows one to generate currents in one spin species by applying forces on the other, and we define

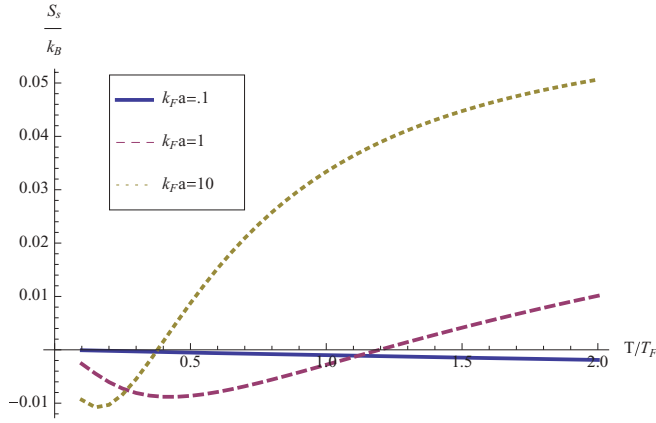


FIG. 2. (Color online) The Seebeck coefficient plotted as a function of the reduced temperature T/T_F , where T_F is the Fermi temperature, for values of $k_F a$ representing weak ($k_F a = 0.1$) and strong ($k_F a = 1$) coupling and approaching the unitary limit ($k_F a = 10$).

a set of spin-heat transport coefficients which captures these effects as follows. We consider a Fermi gas with two different spin states selected from a larger half-integer spin multiplet, which we will call “spin up” (+) and “spin down” (−), for equal spin-up and spin-down densities $n_+ = n_- \equiv n$, i.e., in the absence of spin polarization, and apply equal and opposite forces and temperature gradients for the two spin species, i.e., $\mathbf{F}_+ = -\mathbf{F}_-$ and $\nabla T_+ = -\nabla T_-$. In linear response, the ensuing spin current and spin-heat current defined by $\mathbf{j}_s = \mathbf{j}_+ - \mathbf{j}_-$ and $\mathbf{q}_s = \mathbf{q}_+ - \mathbf{q}_-$, respectively, are given by

$$\begin{pmatrix} \mathbf{j}_s \\ \mathbf{q}_s \end{pmatrix} = \sigma_s \begin{pmatrix} 1 & S_s \\ T S_s & \frac{\kappa_s}{\sigma_s} (1 + Z_s T) \end{pmatrix} \begin{pmatrix} \mathbf{F}_s \\ -\nabla T_s \end{pmatrix}, \quad (1)$$

where $\mathbf{F}_s \equiv \mathbf{F}_+ - \mathbf{F}_-$ is the spin force, $T_s = T_+ - T_-$ is the spin temperature, T is the equilibrium temperature, σ_s is the spin conductivity, κ_s is the spin-heat conductivity (at zero spin current), $Z_s T = \sigma_s S_s^2 T / \kappa_s$, and Onsager reciprocity is explicitly included in the matrix above. We note that \mathbf{F}_s is the thermodynamic force which includes forces coming from pressure gradients, i.e., $\mathbf{F}_s = \mathbf{f}_s^{\text{ext}} - \nabla p_s / n$, where $\mathbf{f}_s^{\text{ext}}$ is the external spin force, and $p_s = p_+ - p_-$ is the difference in pressures of the spin-up and spin-down atoms. These coefficients, computed with the Boltzmann equation described below, are plotted in Fig. 3 as functions of T/T_F for several values of $k_F a$.

As is well known, the spin conductivity σ_s rapidly increases at low temperatures due to Pauli blocking. Our result for σ_s , plotted in Fig. 3(a), includes corrections due to spin-heat coupling, but they are negligibly small, so that one can safely take $\sigma_s = n\tau_s/m$ with τ_s being the spindrag relaxation time [8] measured in Ref. [6] and calculated in Ref. [9]. The downturn of S_s at low temperatures is a quantum mechanical effect that also occurs for bosons, where, in contrast to fermions, the spin conductivity decreases sharply at low temperatures due to bosonic enhancement of scattering [10]. The spin-heat conductivity κ_s is plotted in Fig. 3(b), where it is seen to increase with increasing T . The dimensionless figure of merit $Z_s T$ [Fig. 3(c)] determines the thermodynamic efficiency of engines based on thermo-spin effects [11].

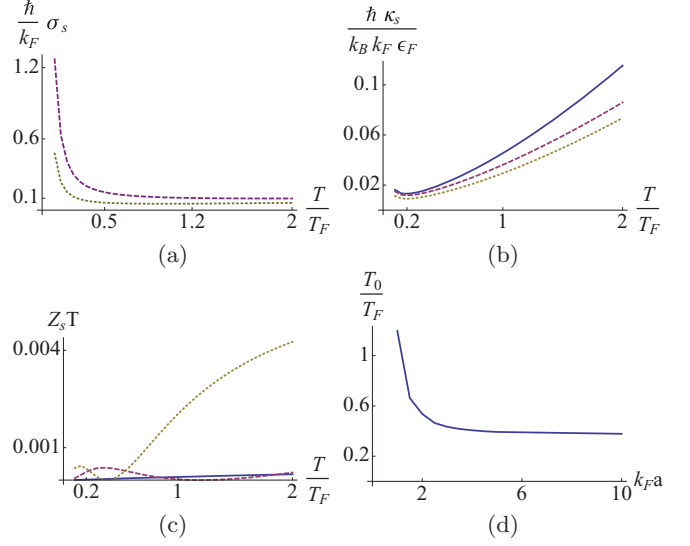


FIG. 3. (Color online) (a) A plot of the spin conductivity normalized as $\hbar \Lambda \sigma_s$, (b) the spin-heat conductivity normalized as $\hbar \Lambda \kappa_s / k_B \epsilon_F$, and (c) the figure of merit $Z_s T$, for $k_F a = 0.1$ (thick blue), $k_F a = 1$ (dashed purple), and $k_F a = 10$ (dotted yellow). (d) A plot of the temperatures T_0 relative to T_F where $S_s = 0$ as a function of $k_F a$.

A spin-dependent temperature gradient can only be established when intraspin scattering is much greater than interspin scattering. For fermions, the first nonvanishing intraspin scattering amplitude is p wave. To make this large, one can tune the p -wave scattering length by a Feshbach resonance [12]. Taking the unitary limit for intraspin scattering, the intra- and interspin differential cross sections are given by

$$\begin{aligned} \frac{d\sigma_{++}}{d\Omega} &= \frac{d\sigma_{--}}{d\Omega} = \frac{9(\hat{\mathbf{p}}_r \cdot \hat{\mathbf{p}}'_r)^2}{(p_r/\hbar)^2}, \\ \frac{d\sigma_{+-}}{d\Omega} &= \frac{a^2}{1 + (p_r a/\hbar)^2}, \end{aligned} \quad (2)$$

where $p_r = |\mathbf{p}_r|$ is the relative momentum of incoming particles with momenta \mathbf{p}_1 and \mathbf{p}_2 , defined by $\mathbf{p}_r = (\mathbf{p}_1 - \mathbf{p}_2)/2$, the hat superscripts denotes unit vectors, and a is the interspin s -wave scattering length.

III. CALCULATION OF TRANSPORT COEFFICIENTS

Next, we present the computation of S_s using the Boltzmann equation. We parametrize the nonequilibrium, steady-state distribution by

$$n_{\mathbf{p}\sigma}(\mathbf{r}) = f_{\mathbf{p}\sigma}(\mathbf{r}) - \partial_\epsilon f_{\mathbf{p}\sigma}^0 \phi_{\mathbf{p}\sigma}(\mathbf{r}), \quad (3)$$

where $f_{\mathbf{p}}^0 = \{\exp[(\epsilon_{\mathbf{p}} - \mu)/k_B T] + 1\}^{-1}$ is the equilibrium Fermi distribution, μ is the chemical potential, $\epsilon_{\mathbf{p}} = \mathbf{p}^2/2m$, $f_{\mathbf{p}\sigma}(\mathbf{r}, t) = \{\exp\{[\epsilon_{\mathbf{p}} - \mu_{\sigma}(\mathbf{r})]/k_B T_{\sigma}(\mathbf{r})\} + 1\}^{-1}$ is the local equilibrium distribution, $\partial_\epsilon f_{\mathbf{p}}^0 = -f_{\mathbf{p}}^0(1 - f_{\mathbf{p}}^0)/k_B T$, and $\phi_{\mathbf{p}\sigma}$ is determined by solving the Boltzmann equation for the spin distribution $n_{\mathbf{p}s} = n_{\mathbf{p}+} - n_{\mathbf{p}-}$ in linear response,

$$\partial_\epsilon f_{\mathbf{p}}^0 \left(\frac{\epsilon_{\mathbf{p}} - w(T)}{k_B T} \right) \mathbf{v}_{\mathbf{p}} = \mathbf{C}_{\mathbf{p}}[\phi], \quad (4)$$

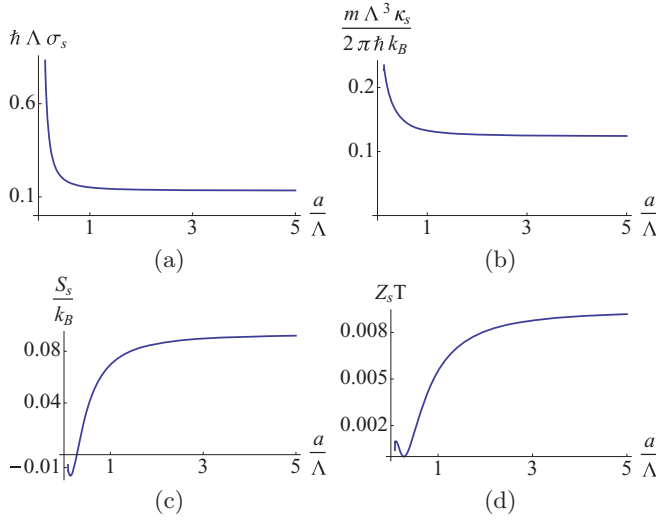


FIG. 4. (Color online) Plots of the transport coefficients in the high-temperature limit, $T \gg T_F$, as a function of a/Λ . (a) The spin conductivity normalized as $\hbar\Lambda\sigma_s$. (b) The spin-heat conductivity normalized as $m\Lambda^3\kappa_s/2\pi\hbar k_B$, (c) S_s/k_B , and (d) $Z_s T$.

where $w(T) = \mu + Ts$ is the enthalpy per particle and s is the entropy per particle [13]. We defined $\phi_{\mathbf{p}s} \equiv k_B\phi_{\mathbf{p}} \cdot (-\nabla T_s)$ and expressed the linearized collision integral in the Boltzmann equation for the spin distribution as $(\partial n_{\mathbf{p}s}/\partial t)_{\text{coll}} \equiv C_{\mathbf{p}}[\phi_{\mathbf{p}}] \cdot (-\nabla T_s)$. The spin current is given by

$$\mathbf{j}_s = - \int \frac{d^3p}{(2\pi\hbar)^3} \partial_\epsilon f_{\mathbf{p}}^0 \mathbf{v}_{\mathbf{p}} \phi_{\mathbf{p}s}. \quad (5)$$

We solve Eq. (4) using the method described in Ref. [5]. Applying the temperature gradient along the x axis, we parametrize the response by a power series,

$$\phi_{\mathbf{p}s}(a, T) = \left[b_0(a, T) + b_1(a, T) \left(\frac{\epsilon_{\mathbf{p}}}{k_B T} \right) \right] p_x (-k_B \partial_x T_s). \quad (6)$$

The coefficients b_0 and b_1 , determined by the approximate solution to Eq. (4), are given by

$$\begin{Bmatrix} b_0(a, T) \\ b_1(a, T) \end{Bmatrix} = \frac{3nl(T)}{C_{00}C_{11} - C_{01}^2} \begin{Bmatrix} -C_{01}(a, T) \\ C_{00}(a, T) \end{Bmatrix}, \quad (7)$$

where

$$l(T) = \frac{35}{4} \frac{f_{7/2}(z)}{f_{3/2}(z)} - \left(\frac{w(T)}{k_B T} \right)^2, \quad (8)$$

$z = e^{\mu/k_B T}$ is the fugacity, $f_n(z) = -\text{Li}_n(-z)$, $\text{Li}_n(z)$ are the polylogarithmic functions, and C_{nm} are the 2×2 matrix elements of the collision integral,

$$\begin{aligned} C_{nm} = & \frac{1}{k_B T} \int \frac{d\mathbf{p}_1 d\mathbf{p}_2}{(2\pi\hbar)^6} \frac{|\mathbf{p}_1 - \mathbf{p}_2|}{m} f_{\mathbf{p}_1}^0 f_{\mathbf{p}_2}^0 \\ & \times \frac{1}{4} \int d\Omega_r (1 - f_{\mathbf{p}_3}^0)(1 - f_{\mathbf{p}_4}^0) \\ & \times \sum_{\sigma=\pm} \left\{ \frac{d\sigma_{+\sigma}}{d\Omega_r} \Delta_{+\sigma} [(\epsilon_{\mathbf{p}}/k_B T)^n \mathbf{p}] \cdot \Delta_{+\sigma} [(\epsilon_{\mathbf{p}}/k_B T)^m \mathbf{p}] \right\}, \end{aligned} \quad (9)$$

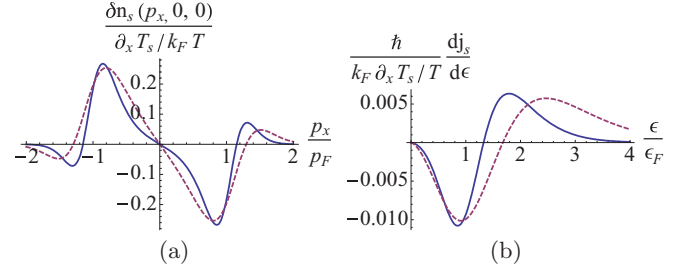


FIG. 5. (Color online) A plot of (a) the perturbed spin distribution per spin temperature gradient, normalized as $\delta n_s/(-\partial_x T/k_F T)$ along the p_x axis. A plot of (b) the spin current density along the p_x axis, per $d\epsilon$ per spin temperature gradient, normalized as $(dj_s/d\epsilon)(\hbar/k_F)(\partial_x T_s/T)$, for $k_F a = 10$ and temperatures at which S_s is negative ($T = 0.3T_F$, blue thick line) and positive ($T = 0.5T_F$, purple dashed line).

where we define $\Delta_{++}[\phi_{\mathbf{p}}] = \phi_{\mathbf{p}_3} + \phi_{\mathbf{p}_4} - \phi_{\mathbf{p}_1} - \phi_{\mathbf{p}_2}$ and $\Delta_{+-}[\phi_{\mathbf{p}}] = \phi_{\mathbf{p}_3} - \phi_{\mathbf{p}_4} - \phi_{\mathbf{p}_1} + \phi_{\mathbf{p}_2}$ for an arbitrary function $\phi_{\mathbf{p}}$, and in the integrand momentum conservation is satisfied: $\mathbf{p}_1 + \mathbf{p}_2 = \mathbf{p}_3 + \mathbf{p}_4$.

From Eqs. (5), (6), and (1), it follows that the Seebeck coefficient is given in terms of b_0 and b_1 , and the spin conductivity σ_s by

$$S_s(a, T) = \frac{n}{\sigma_s} \left[b_0(a, T) + b_1(a, T) \frac{w(T)}{k_B T} \right]. \quad (10)$$

The other transport coefficients are calculated similarly. In order to make the numerics more tractable, we have omitted the angular dependence in $d\sigma_{++}/d\Omega$ [c.f. Eq. (2)]. On the other hand, in the high-temperature limit, the integrals in Eq. (9) including the angular factor can be done analytically [14], which allows us to calculate the coefficients in the high-temperature limit. The result is shown in Fig. 4 plotted as a function of a/Λ , where $\Lambda = \sqrt{2\pi\hbar^2/mk_B T}$ is the thermal deBroglie wavelength. In this limit, the dependence of σ_s on the scattering length a can be understood from classical considerations. The spin conductivity is approximately related to the interspin collision time τ_{+-} by $\sigma_s \propto n\tau_{+-}$ and $1/\tau_{+-} = n\bar{\sigma}_{+-}v_T$, where $\bar{\sigma}_{+-}$ is the interspin cross section and $v_T \propto 1/\Lambda$ is the average thermal velocity. In the limit $a/\Lambda \rightarrow 0$, $\bar{\sigma}_{+-} \propto a^2$, thus $\Lambda\sigma_s \propto (\Lambda/a)^2$, and when $a/\Lambda \rightarrow \infty$, $\bar{\sigma}_{+-} \propto \Lambda^2$, thus $\Lambda\sigma_s \propto 1$, in agreement with our result.

The behavior of the transport coefficients depends crucially on the shape of the perturbed spin distribution $\delta n_{\mathbf{p}s} = -\partial_\epsilon f_{\mathbf{p}}^0 \phi_{\mathbf{p}s}$ and the associated spin current density, which we plot for $k_F a = 10$ in Fig. 5. The positive (negative) parts of $\delta n_{\mathbf{p}\sigma}$ may be regarded as particles (holes) having group velocities $\pm\mathbf{p}/m$. Since $\delta n_{\mathbf{p}\sigma} = -\delta n_{\mathbf{p}-\sigma}$, every spin-up particle is matched with a spin-down hole with the same momentum, resulting in the spin current. Thus, the sign of S_s is determined by the relative number of particles or holes induced in response to the spin temperature gradient.

Next, we give a criterion that determines the sign of the spin-Seebeck coefficient and show that it does not depend on the form of the intraspin scattering at all. First, we note that in our solution given by Eq. (7), we always have $b_0 < 0$ and $b_1 > 0$ because $l(T) > 0$, $C_{nm} > 0$, and $\det \hat{C} > 0$ [15]. Thus for positive momenta, b_1 (b_0) corresponds to particles (holes)

created above (below) the Fermi surface. Inspecting Eq. (10), we find that the criteria to have $S_s \leq 0$ is

$$\left| \frac{b_0}{b_1} \right| = \left| \frac{C_{01}}{C_{00}} \right| \geq \frac{w}{k_B T} \quad (11)$$

and the opposite inequality for $S_s > 0$. Thus S_s is positive when b_1 becomes large enough to violate Eq. (11) [16]. Furthermore, it turns out that the only integral in Eq. (9) containing intraspin scattering that is nonvanishing is C_{11} , which does not enter in Eq. (11).

The temperature dependence of b_0 and b_1 follows from the temperature dependence of the collision matrix elements in Eq. (9), which are given by integrals nonvanishing only for $p_r \sim \sqrt{4\pi\hbar}/\Lambda$. Therefore, it is useful to express the differential cross section Eq. (2) in terms of the rescaled momentum $\tilde{p}_r = (\Lambda/\sqrt{4\pi\hbar})p_r$,

$$\frac{d\sigma_{+-}}{d\Omega} = \frac{1}{k_F^2} \frac{(k_F a)^2}{1 + (k_F a)^2 (T/T_F) \tilde{p}_r}. \quad (12)$$

From Eq. (12) we see that the change in the sign of S_s is related to the crossover from hard-sphere scattering, $d\sigma/d\Omega \simeq$

a^2 , when $k_F a \ll 1$ or $T/T_F \ll 1$, to momentum-dependent scattering, $d\sigma/d\Omega \sim \tilde{p}_r^{-2}$, when $k_F a \simeq 1$ and $T \simeq T_F$.

IV. DISCUSSIONS AND OUTLOOK

We note that as the temperature is lowered, one expects to enter the Fermi-liquid regime, for $T_c < T \ll T_F$, where T_c is the temperature for the superfluid transition, and one should use Fermi-liquid scattering amplitudes in the collision integral [9]. Near and above T_c , one should also take into account the effects of pairing correlations on the interspin interaction [17]. Both these regimes can be analyzed with the formalism presented in this paper and will be relegated to future work.

ACKNOWLEDGMENTS

This work was supported by Stichting voor Fundamenteel Onderzoek der Materie (FOM), the Netherlands Organization for Scientific Research (NWO), and the European Research Council (ERC) under the Seventh Framework Program (FP7).

-
- [1] G. E. W. Bauer, A. H. MacDonald, and S. Maekawa, *Solid State Communications* **150**, 459 (2010).
 - [2] M. Hatami *et al.*, *Solid State Commun.* **150**, 480 (2010); C. M. Jaworski *et al.*, *Nat. Mater.* **9**, 898 (2010); A. Slachter *et al.*, *Nat. Phys.* **6**, 879 (2010).
 - [3] Y. J. Lin, K. Jimenez-Garcia, and I. B. Spielman, *Nature (London)* **471**, 83 (2011); T. D. Stanescu, C. Zhang, and V. Galitski, *Phys. Rev. Lett.* **99**, 110403 (2007).
 - [4] R. A. Duine and H. T. C. Stoof, *Phys. Rev. Lett.* **103**, 170401 (2009).
 - [5] C. H. Wong, H. J. van Driel, R. Kittinaradorn, H. T. C. Stoof, and R. A. Duine, *Phys. Rev. Lett.* **108**, 075301 (2012).
 - [6] A. Sommer *et al.*, *Nature (London)* **472**, 201 (2011).
 - [7] R. Meppelink, R. van Rooij, J. M. Vogels, and P. van der Straten, *Phys. Rev. Lett.* **103**, 095301 (2009).
 - [8] We note that the measured values of the transport coefficients should be compared with the trap-averaged values, which differ slightly from the results presented here, but may readily be computed using our Boltzmann formalism.
 - [9] G. M. Bruun, *New J. Phys.* **13**, 035005 (2011).
 - [10] H. J. van Driel, R. A. Duine, and H. T. C. Stoof, *Phys. Rev. Lett.* **105**, 155301 (2010).
 - [11] G. Mahan, *Solid State Physics* (Academic Press, San Diego, 1997), Vol. 51, pp. 81–157.
 - [12] C. A. Regal, C. Ticknor, J. L. Bohn, and D. S. Jin, *Phys. Rev. Lett.* **90**, 053201 (2003); K. B. Gubbels and H. T. C. Stoof, *ibid.* **99**, 190406 (2007).
 - [13] Since $s \sim T/T_F$, for degenerate fermions, one usually takes $w \rightarrow \mu$.
 - [14] Specifically, C_{nm} can be expressed in terms of incomplete Γ functions.
 - [15] The eigenvalues of the collision matrix are negative because they correspond to relaxation times, and therefore, for the 2×2 collision matrix, the determinant must be positive.
 - [16] Note that the Seebeck coefficient vanishes in a simple relaxation time approximation given by $\phi_{ps} = \tau_s(w - \epsilon_p)v_x \partial_x T_s/T$, corresponding to the case $b_0/b_1 = w/k_B T$ in Eq. (11).
 - [17] G. M. Bruun and H. Smith, *Phys. Rev. A* **72**, 043605 (2005).